Nanotechnology Perceptions
ISSN 1660-6795
www.nano-ntp.com

Voltage Stability Enhancement of Self-Excited Induction Generator based Wind Energy System using Closed Loop Control of STATCOM

Venu Yarlagadda, V. Ramesh Babu, Venu Yarlagadda, ShashivardhanBagari

EEE Dept, VNR Vignana Jyothi Institute of Engineering and Technology, Hyderabad, India
Email: venu_y@vnrvjiet.in

Modern power system have many interconnections are prone to voltage instability particularly when an electric grid is integrated with renewable energy resources. This study aims to design and development of wind farm based single machine load bus (SMLB) test system for presenting case study and result analysis. The SMLB system is more suitable for voltage stat ability analysis, this article is focused on the design and develop of a wind farm based SMLB system equipped with self-Excited Induction Generator (SEIG) with the shunt capacitor for self-excitation and integrated with a closed loop controlled STATCOM for enhancing its voltage stability and subsequently for controlling voltage profile within the tolerable limits. Additionally, the impact of STATCOM control strategies on voltage stability and system performance has been investigated. The SMLB test system with wind farm has been designed and developed for presenting case study and result analysis. The SMLB system has been simulated without and with open loop control and closed loop control of STATCOM and presented the results with PV curves and voltage bar charts. The results demonstrate the significant improvement in voltage stability achieved through the integration of a STATCOM, highlighting its role in enhancing the reliability and voltage stability of SEIG-based wind energy systems. This analysis provides valuable insights for the design and operation of wind power generation systems with improved voltage stability characteristics

1. Introduction

The increasing demand for renewable energy sources, coupled with growing concerns about environmental sustainability, has led to the widespread adoption of wind energy systems

worldwide. Self-excited induction generators (SEIGs) are commonly used in small to medium-scale wind energy applications due to their simplicity, robustness, and cost-effectiveness. However, SEIG-based wind energy systems face challenges related to voltage stability, particularly under varying wind conditions and fluctuating loads [1]-[2]. Voltage instability can lead to voltage collapse, equipment damage, and disruption of power supply. Static Synchronous Compensators (STATCOMs) have emerged as effective solutions for voltage control and reactive power compensation in power systems. By injecting or absorbing reactive power as needed, STATCOMs can regulate voltage and improve system stability [5] to [6].

I.1. This article presents the work flow in the following chapters

Chapter 2: Deals with the formation of the SMLB test system, which is equipped with the wind turbine coupled to the self-excited induction generator supported with the three-phase delta connected capacitor bank and a static synchronous compensator (STATCOM) for enhancing its voltage stability and subsequently controlling its terminal voltage within the tolerable limit. The SMLB system formation is explained in the second chapter of this article. The Voltage stability is an important aspect of the power system security with the penetration of the renewable resources. The wind farm is an important contributor of renewable energy systems and it is used to form a single machine load bus (SMLB) test system, which is used to evaluate the system voltage stability and subsequently power system security. The SMLB test system is designed and developed using wind farm with the support of shunt capacitors for the self-excitation mechanism, which is described in the second chapter of this article [4] to [6].

Chapter3: Emphasizes the wind turbine modeling [5] to [8].

Chapter 4: Deals with the detailed description of SEIG and its design also it emphasizes the mathematical modelling of SEIG. Further it also deals with the capacitance design for the self-excitation process using magnetization characteristics of the Induction machine [1] to [6].

Chapter 5: Presents the working and mathematical modeling of STATCOM and its design for voltage regulation and to ensure voltage stability of SMLB test system formed with wind farm [10] to [13].

Chapter 6: Highlights the voltage stability and active power margins for security with the use of PV curves [3] to [8].

Chapter 7: Emphasizes the evaluation of the voltage stability characteristics of SEIG-based wind energy systems, investigate the impact of open loop and closed loop control of STATCOM on voltage regulation, and evaluate the effectiveness of STATCOM in enhancing the voltage stability. Comprehensive voltage stability analysis of SEIG-based wind energy systems with the integration of STATCOM has been presented with voltage waveforms, tabular forms and PV curves without and with open loop control and closed loop controlled STATCOM followed by conclusions and references[12] to [13].

2. System Description

This articledeals with the design and development of wind farm based single machine load bus (SMLB) test system for presenting case study and result analysis. The Fig.1 illustrates the

wind energy system with capacitor bank and STATCOM, capacitor bank supplies required leading current, Ic1 to the SEIG for ensuring self-excitation process and STATCOM is supplying required leading current Ic2 to the load in order to control the terminal voltage subsequently to enhance voltage stability margin. The test system is formed with various components to feed the isolated resistive and inductive load with a power factor of 0.89 lagging. The wind turbine has been developed with a wind speed of 24 m/s velocity and a base speed of 1.05p.u. and a pitch angle of 15°. The Induction Generator of squirrel cage type with the following specifications of with rating of 5HP with a voltage of 460V, frequency of 60Hz and speed of 1750 r.p.m inbuilt model. The delta connected three phase capacitor bank is designed and developed to ensure self-excitation phenomenon of SEIG using its magnetisation characteristics. The designed value of the per phase capacitance of delta connected capacitor bank for the self-excitation is of 75μF, further a three phase GTO based STATCOM of 7.5KVAr is designed and connected to the wind farm to improve its voltage stability against inductive load variations as illustrated in the following Fig.1 The SMLB [6] to [13].

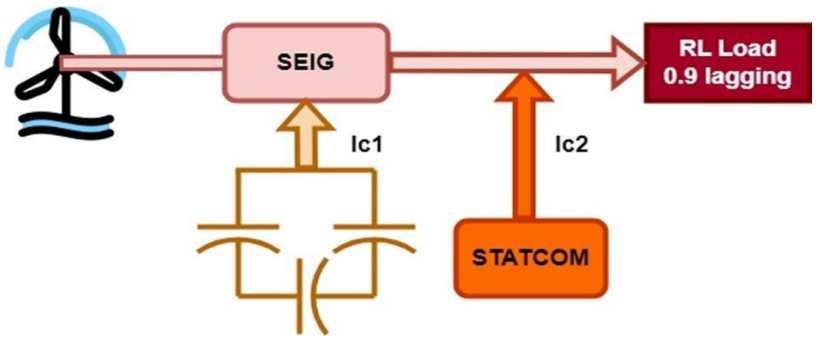

Figure.1. Wind energy system with capacitor bank and STATCOM

3. Mathematical modelling of Wind Turbine

Wind turbine is a basic component of the wind plant and the mechanical power is expressed in Equation (1) and Fig.2. Shows the Wind turbine Generator set and equations from (2) to (12) describe its mathematical modelling. Equation (2) describes the kinetic energy and equation (3), (4) describes the wind power, equation (5) depicts the turbine blade power, tip speed is shown by the equation (6). Equation (7) presents the wind torque in terms of blade power and other parameters and remaining equations from (8) to (12) describes the complete wind turbine model [5], [13].

$$P = 0.5 * C_P(\lambda, \beta)\rho A\,(v)^3 \quad (1)$$

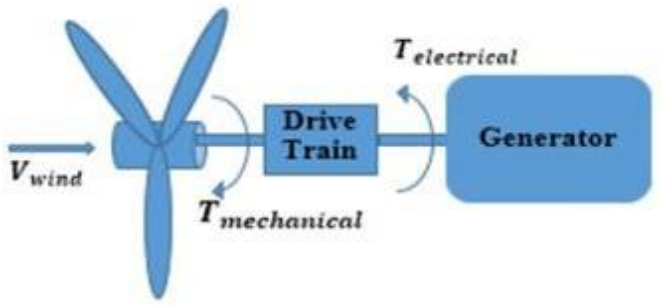

Figure.2 Wind turbine Generator set

$$E = \frac{1}{2}mv^2 \quad (2)$$

$$\frac{dE}{dt} = \frac{1}{2}mv \quad (3)$$

$$P_w = \frac{1}{2}m\rho v^3 \quad (4)$$

$$P_{Blade} = C_p(\lambda,\beta)P_w = C_p(\lambda,\beta)\frac{1}{2}m\rho v^3 \quad (5)$$

$$\lambda = \omega mRv \quad (6)$$

$$T_W = \frac{P_{Blade}}{\omega_m} = \frac{\pi C_P(\lambda,\beta)\,\rho R^2 A V^3}{\omega_m} \quad (7)$$

$$C_P(\lambda,\beta) = C_1\left(C_2\frac{1}{\nu} - C_3\beta - C_4\beta^{\nu} - C_5\right)e^{-C_6\frac{1}{\gamma}} \quad (8)$$

$$T_W = \frac{1}{2}(C_P(\lambda,\beta)\rho A V^3) \quad (9)$$

$$C_P = 0.22\left(\frac{116}{\gamma} - 0.4\beta - 5\right)e^{\frac{-12.5}{\gamma}} \quad (10)$$

$$\frac{1}{x} = \frac{1}{(\lambda - 0.08\beta)} - \frac{0.035}{(1+\beta^3)} \quad (11)$$

$$\lambda = \frac{wR}{v} \quad (12)$$

4. Self-Excited Induction Generator (SEIG)

4.1 Working of SEIG

Induction machine always demand necessary reactive power support for its satisfactory functioning, whether it is acting as a generator or a motor. The necessary reactive power for the self- excitation of squirrel cage Induction Generator is achieved with the support of delta connected three phase capacitor banks connected in parallel to the stator of SEIG as illustrated with the following Fig.23. Due to residual magnetism, a significant voltage is produced

between the stator terminals when the rotor rotates at significantly higher than the critical speed. This low generated voltage drives the capacitor current, which enhances the magnetization current and produces more reactive power and it continues till machine excites to its rated voltage like in d.c. machine. The developed system operates in an isolated mode; hence a self-excited induction generator is the best choice for this model and the Fig.3 illustrating the Self-Excited Induction Generator with Capacitor Bank. The fig.4. Torque Slip characteristics of Induction Machine [1]-[5].

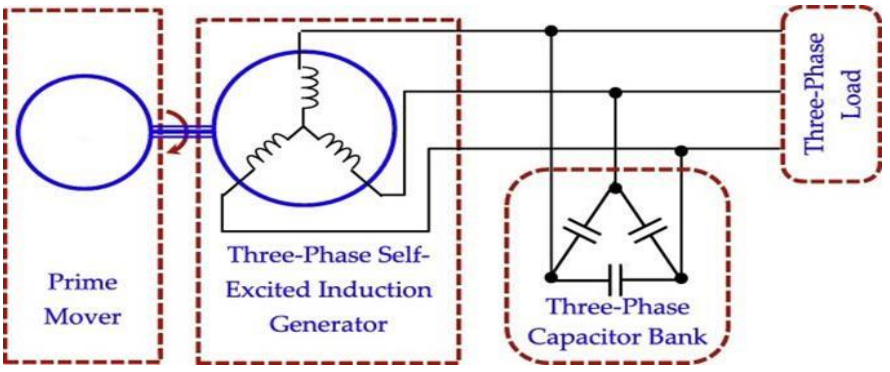

Figure.3. Self-Excited Induction Generator with Capacitor Bank

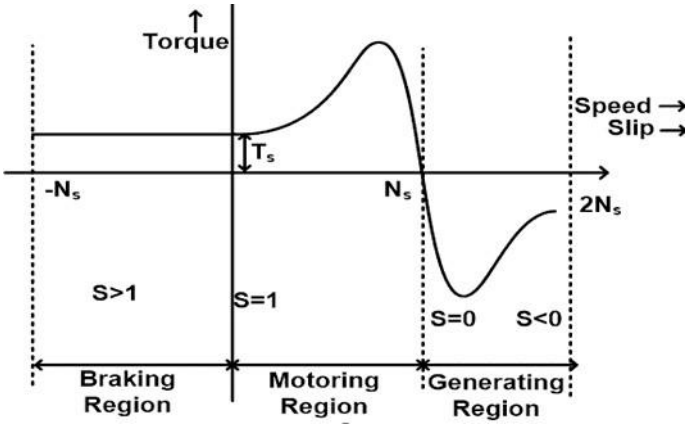

Figure.4. Torque Slip characteristics of Induction Machine

4.2 Design of delta connected capacitor bank for SEIG

A single-phase equivalent circuit of SEIG as shown in Fig.5 is called a negative resistance oscillator. Fig.6 shows magnetisation characteristics of an induction generator and is used to compute the required capacitance value for self-excitation process where the capacitance value, below which the generator will fail to build-up voltage, called critical capacitance value of C3 [3] to [8].

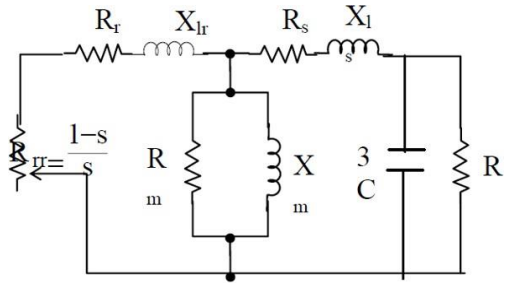

Figure.5. Single-phase equivalent circuit of SEIG

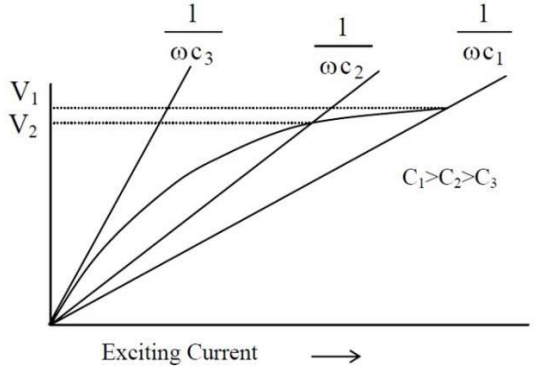

Figure.6. Magnetisation Characteristics of SEIG

4.3 Mathematical Modelling of SEIG

Asynchronous generator equations have been described below and it is operating in negative torque-slip region. Equations (13) to (32) describe the mathematical modeling of the Asynchronous Generator used as self-excited wind generator. The stator side voltage equations are described from equations (13) to (15), stator flux linkage equations are expressed from equations (16) to (20), the rotor side voltage equations have been expressed in the following equations (21) to (24), rotor flux linkage equations have been described from the following equations from (25) to (31) and finally the torque equation described by the equation (32) [4] to [7].

Stator Side Equations have been presented the following set of equations from (13) to (20)

$$V_{as} = r_s i_{as} + \frac{d\lambda_{as}}{dt} \quad (13)$$

$$V_{bs} = r_s i_{bs} + \frac{d\lambda_{bs}}{dt} \quad (14)$$

$$V_{cs} = r_c i_{as} + \frac{d\lambda_{cs}}{dt} \quad (15)$$

$$V^{a}_{abcs} = r_s (i^{a}_{abcs}) + \frac{d\lambda^{a}_{abcs}}{dt} \quad (16)$$

$$\lambda_{as} = L_{1s} i_{as} + M(i_{as} + i'_{ar}) \quad (17)$$

$$\lambda_{bs} = L_{1s} i_{bs} + M(i_{bs} + i'_{\beta r}) \quad (18)$$

$$\lambda_{cs} = L_{1s} i_{cs} + M(i_{cs} + i'_{\gamma r}) \quad (19)$$

$$\lambda^{a}_{abcs} = (L_s + M)(i^{a}_{abcs}) + L_{sr}(i^{a}_{abcr}) \quad (20)$$

Rotor side equations have been presented the following set of equations from (21) to (30) and flux linkage and torque equations have been expressed with subsequent equations (31) and (31) respectively and equation (32) describes the electrical power equivalent torque of the SEIG, which enables the machine to produce necessary active power to feed the loads [6] to [13].

$$0 = r'_r (i'^{a}_{r\ abcr}) + \frac{d\lambda'_{ar}}{dt} + \frac{(\lambda'_{\beta r} - \lambda'_{\gamma r})}{\sqrt{3}} \quad (21)$$

$$0 = r'_r (i'^{a}_{r\ abcr}) + \frac{d\lambda'_{\beta r}}{dt} + \frac{(\lambda'_{\gamma r} - \lambda'_{ar})}{\sqrt{3}} \quad (22)$$

$$0 = r'_r (i'^{a}_{r\ abcr}) + \frac{d\lambda'_{\gamma r}}{dt} + \frac{(\lambda'_{ar} - \lambda'_{\beta r})}{\sqrt{3}} \quad (23)$$

$$0 = r'_r (i'^{a}_{r\ abcr}) + \frac{d[\lambda'^{a}_{abcr}]}{dt} \quad (24)$$

$$\lambda^{a}_{abcr} = (L_r + M)(i^{a}_{abcs}) + L_{sr}(i^{a}_{abcs}) \quad (25)$$

$$\lambda'_{ar} = L'_{lr} i'_{ar} + M(i_{as} + i'_{ar}) \quad (26)$$

$$\lambda'_{\beta r} = L'_{lr} i'_{\beta r} + M(i_{bs} + i'_{\beta r}) \quad (27)$$

$$\lambda'_{\gamma r} = L'_{lr} i'_{\gamma r} + M(i_{cs} + i'_{\gamma r}) \quad (28)$$

$$\lambda^{a}_{abcr} = (L_r + M)(i^{a}_{abcs}) + L_{sr}(i^{a}_{abcs}) \quad (29)$$

$$\lambda'^{a}_{abcr} = (L'_{lr} + M)[i'^{a}_{abcs}] + [L_{lr}]^T [i^{a}_{abcs}] \quad (30)$$

$$\frac{d[\lambda'_{a\beta\gamma r}]}{dt} = L_{lr} \frac{d[i'_{a\beta\gamma r}]}{dt} + M \frac{d[i_{abcm}]}{dt} + [i_{abcm}] \frac{dM}{dt} \quad (31)$$

$$T_e = \frac{2}{p} J \frac{dw_r}{dt} + \frac{2}{p} B_m w_r + T_L \quad (32)$$

5. STATCOM

5.1 Working of GTO based STATCOM

STATCOM is a shunt connected device which employs GTO's as depicted in Fig.7, which is basically fast acting switching device in order to improve stability of power system. The Fig.8illustratesits V-I Characteristics of STATCOM VI characteristics depicts that the STATCOM [10] to [13].

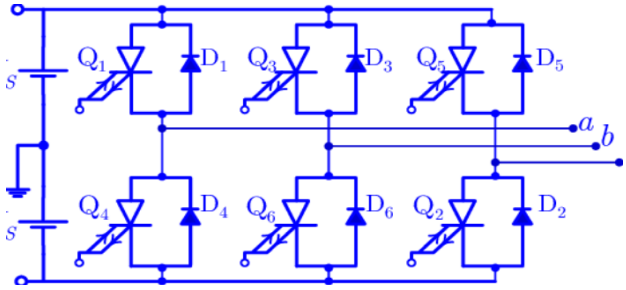

Figure.7 GTO based STATCOM Schematic diagram

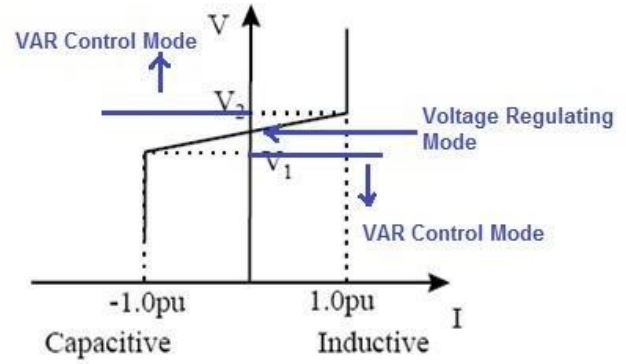

Figure.8 V-I Characteristics of STATCOM

5.2 Mathematical Modelling of STATCOM

The following equations from (33) to (37) describes the mathamatical modelling of STATCOM, for active power, reactive power of STATCOM are as follows in equations (33) and (34), remaining equations describes the voltage equations of STATCOM [11] to [13].

$$P = \frac{V_t V_C}{X_L} \sin \alpha \tag{33}$$

$$Q = \frac{V_t V_t}{X_L} - \frac{V_t V_C}{X_L} \cos \alpha \tag{34}$$

$$L \frac{di_{ac}}{dt} = R i_{ac} + V_{ac} - V_{at} \tag{35}$$

$$L \frac{di_{bc}}{dt} = R i_{bc} + V_{bc} - V_{bt} \tag{36}$$

$$L \frac{di_{cc}}{dt} = R i_{cc} + V_{cc} - V_{ct} \tag{37}$$

The wind energy conversion system is formed with a wind turbine, SEIG excited with a three-phase delta connected capacitor bank designed with excitation characteristics and GTO based STATCOM to enhance voltage stability and to regulate its terminal voltage against load disturbances. This system forms a single machine load bus system (SMIB) system with a wind power plant. The SMLB system is usually most suitable system for the study of voltage stability against faults and load variations. The most power full tool for assessing voltage stability of SMLB system is power-voltage (PV) curves, which is drawn between load power versus terminal voltage of the SMLB test system. Fig.9illustratrates the PV curve of an SMLB system, where voltage is plotted on the y-axis against power variations taken on the x-axis, voltage is dependent parameter on the power variations from very low value to a significantly very high value. This PV curve is also known as the nose curve of the SMLB system since it look like a human nose at nose point dV/dP is equal to zero and it is a condition for voltage stability and system is critically or marginally stable up to this point. When dV/dP is negative the voltage falls down with the increase of the power demand and system is completely stable with λ as the available secured power margin also known as security loading level. The available secured power margin, λ is determined from the PV curve as illustrated in the following Fig.9, is the active power distance measured on the x-axis from base case loading level (PD) to security loading level (PDSL). The complete voltage stability margin (VSM), which is the maximum possible active power margin is determined from the active power distance measured on the x-axis from base case loading level (PD) to voltage collapse point (VSM). Beyond the critical point or nose point the system is unstable and dV/dP is positive i.e. the voltage falls down and generator power also falls down simultaneously leads to voltage instability subsequently voltage collapse. The voltage band between Vmin and Vmaxas illustrated in the Fig.9 is the required voltage regulation of the SMLB system, hence the focus of the article is to maintain the voltage stability by integrating the voltage control in the specified band as depicted in the following Fig.9 [4] to [13].

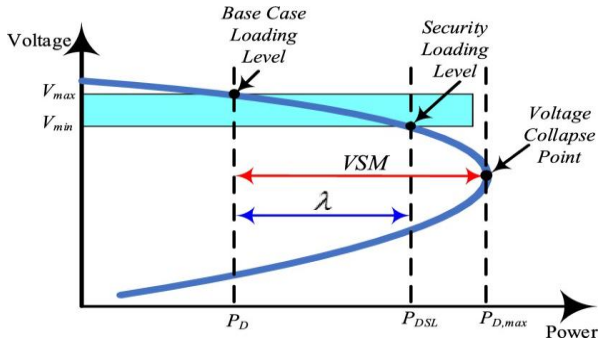

Figure.9. PV curve of an SMLB system

7. Case Study and result Analysis

The SMLB system has been formed with a wind farm equipped with wind turbine and inputs to wind turbine are wind speed and pitch angle, and it is mechanically coupled to the SEIG through a gearbox to ensure necessary speed for self-excitation. The SEIG is provided with three phase delta connected capacitor bank to ensure self-excitation process designed from its

excitation characteristics explained in the earlier section of this article. Further this system is equipped with the three phase GTO based STATCOM to control the terminal voltage and to ensure the voltage stability of the SMLB system. The said system is designed and developed for the case study in two major parts, one is without STATCOM and second is with STATCOM. The system is simulated and presented results without and with STATCOM, the terminal voltage waveforms and PV curves of the system in both the parts have been presented in the following sections.

7.1 Case I: wind energy system without STATCOM

The SMLB test system has been designed and developed with wind plant without STATCOM but self-excitation is designed using excitation characteristics as described in earlier section of this article. Fig.10 illustrated the SEIG based Wind plant with a delta connected 3-ph Capacitor bank. The per unit speed of the wind turbine is 1.05 p.u., pitch angle of 24 degrees and wind speed of 15 m/s has been taken and a 3-phase delta connected capacitor bank of 75μF of per phase capacitance is designed and connected across the stator terminals as illustrated in the following Fig.10, feeding an inductive load with a power factor of 0.89 lagging. The simulation of the system is carried out with the designed values and presented the results without STATCOM. the first part of this section presents the terminal voltage waveforms under different inductive loads with a constant power factor of 0.89 lagging. Fig.11 shows the voltage waveforms for RL Load 1, Fig.12 depicts the voltage waveforms for RL Load 2, Fig.13 portrays the voltage waveforms for RL Load 3, Fig.14 illustrates the voltage waveforms for RL Load 4 and finally Fig.15represents the voltage waveforms for RL Load 5. Table 1 encapsulates the terminal voltages of system without STATCOM and Fig.16 presents its PV Curve, which indicates the more voltage dip due to change in inductive load and it is highly undesirable as par as voltage stability is a concern and also not acceptable in the voltage regulation point of view.

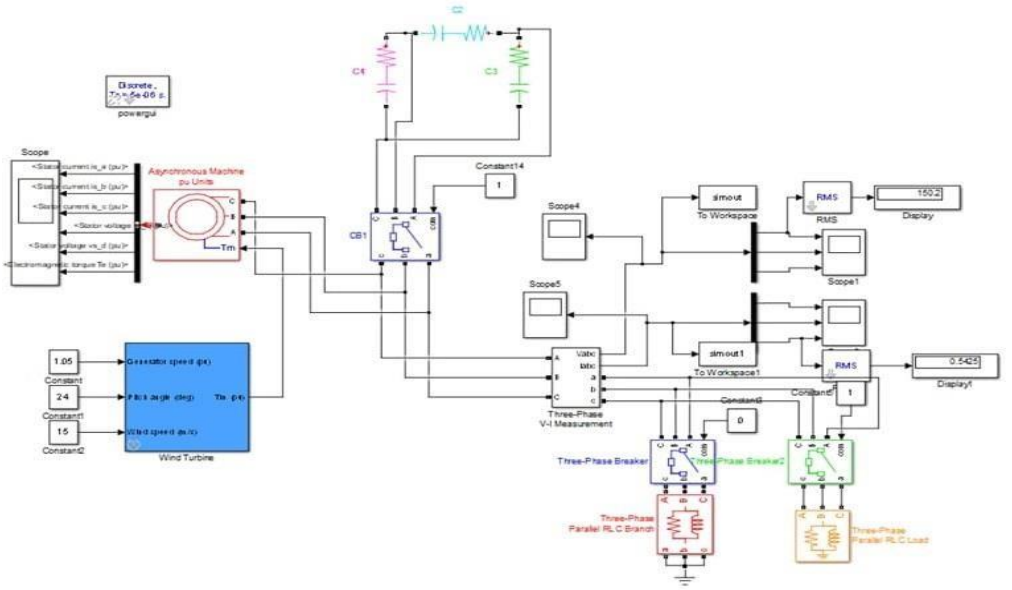

Figure.10. SEIG based Wind plant with a delta connected 3-ph Capacitor bank

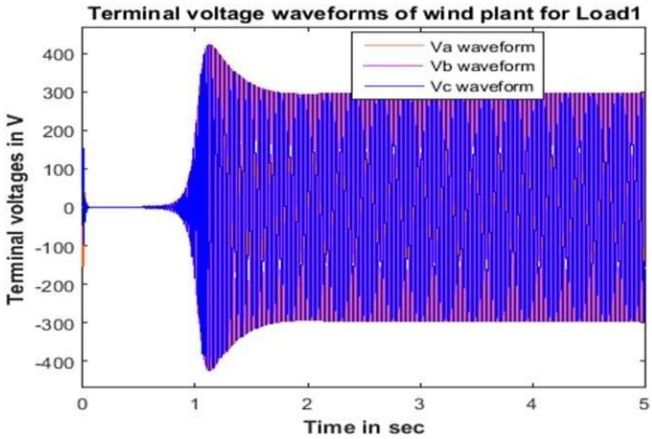

Figure.11. Voltage waveforms for RL Load 1

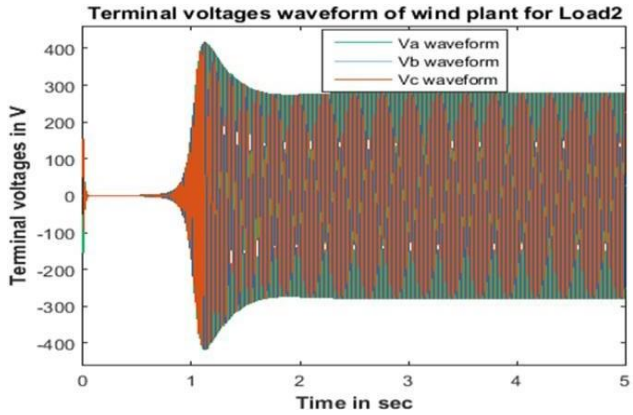

Figure.12. Voltage waveforms for RL Load 2

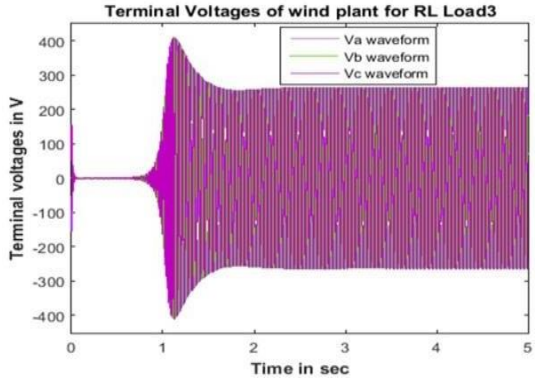

Figure.13. Voltage waveforms for RL Load 3

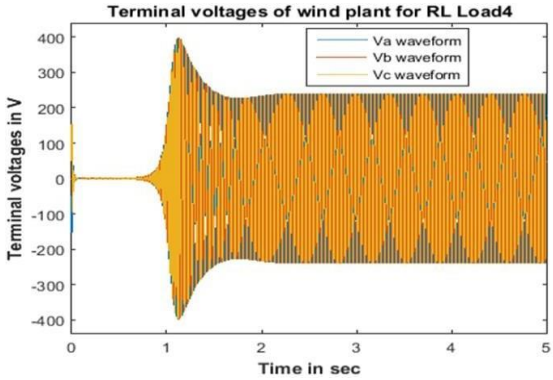

Figure.14. Voltage waveforms for RL Load 4

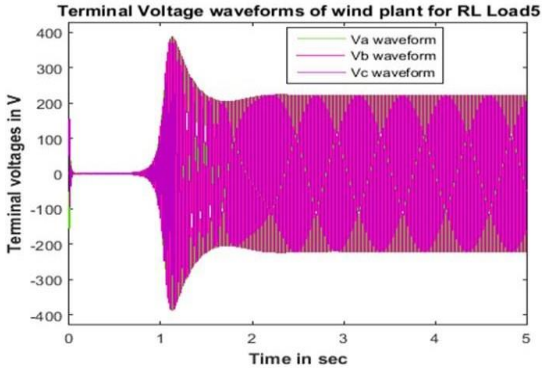

Figure.15. Voltage waveforms for RL Load 5

Parameter	No Load	RL Load 1	RL Load 2	RL Load 3	RL Load 4	RL Load 5	RL Load 6	RL Load 7	RL Load 8
Active T aPower P bin W	0	250	500	750	1000	1250	1500	1750	2000
lReactive ePower Q in VAr	0	125	250	375	500	625	750	875	1000
1 :Voltage in V	250	194.1	173	162.5	169.1	181.9	180.8	157.9	132.4

Terminal voltages of system without STATCOM

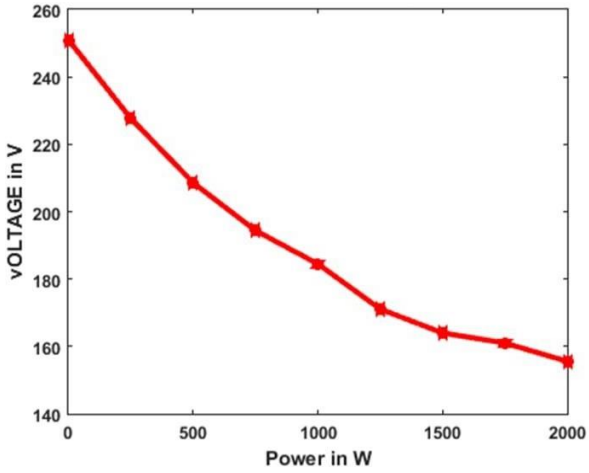

Figure.16. PV Curve without STATCOM

7.2 Case II: wind energy system with STATCOM

This part of the case study and result analysis have been performed with a delta connected three phase capacitor banks, which ensures the self-excitation of SEIG and a STATCOM, which ensures the voltage regulation of the system and its voltage stability against load disturbances. The following section has presented the terminal voltage waveforms and PV curves with STATCOM. The results of the system have been presented in two modes, one is open loop control and the second is the closed loop control mode of the STATCOM.

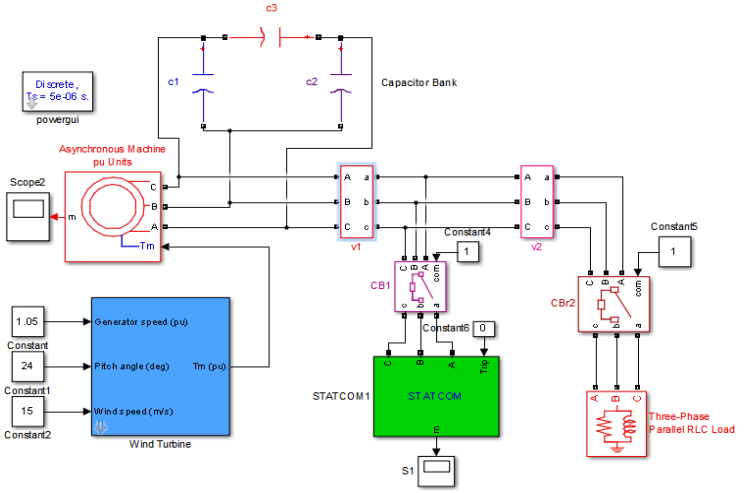

Figure.17. SEIG based Wind plant with Capacitor bank and STATCOM

7.3 Case II. 1 Open loop Control of the STATCOM

The first part of this result analysis section presents the case study of the system with the design and development of the STATCOM including passive filters used to mitigate the injected

harmonics. This part presents the open loop control results of the STATCOM. Table 2 encapsulates the terminal voltages of system with open loop control of STATCOM and Fig.18 shows the PV curves of the system without and with open loop control of STATCOM and Fig.19. Bar chart of voltages with open loop control of STATCOM. These results clearly proven the fact with the open loop control of STATCOM the voltage stability has been enhanced tremendously with effective voltage regulation in the specified band.

Table 3: Terminal voltages of system with closed loop control of STATCOM

Parameter	No Load	RL Load 1	RL Load 2	RL Load 3	RL Load 4	RL Load 5	RL Load 6	RL Load 7	RL Load 8
Active Power P in W	0	250	500	750	1000	1250	1500	1750	2000
Reactive Power Q In VAR	0	125	250	375	500	625	750	875	1000
Voltage IN V	232	231.3	231.2	231	230.9	230.7	230.5	230.4	230.2

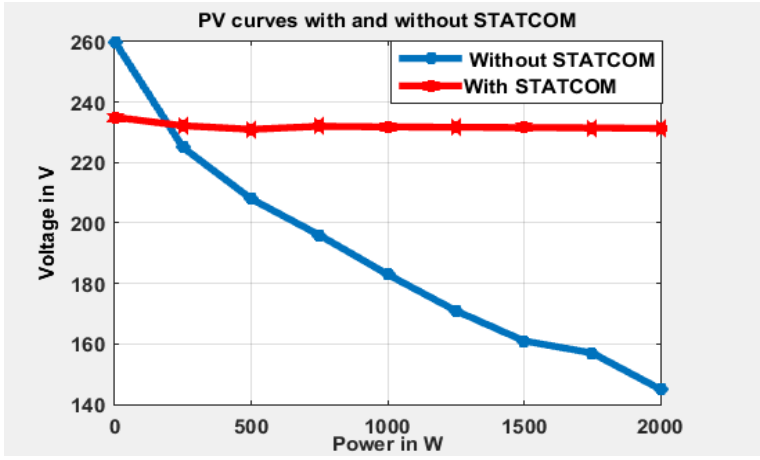

Figure.18. PV curves of the system without and with open loop control of STATCOM

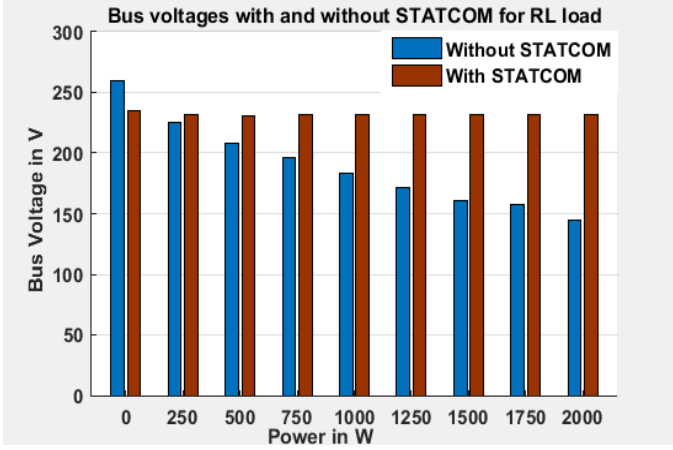

Figure.19. Voltages with open loop control of STATCOM

7.4 Case II. 2Closed loop Control of the STATCOM

This part of the result analysis presents the system results with the closed loop control of STATCOM and subsequent part reveals the comparative analysis of system results without and with STATCOM. Fig 20 shows the STATCOM Closed loop control circuit, the terminal voltage of the system VL is passed through a proper gain and is considered to generate synchronizing signals through the phase locked loop (PLL). This terminal voltage VL is transformed in to direct axis and quadrature axis voltages using park's transformation, which transforms ac signals into dc values. The digital PI controller is designed and implemented in the control circuit of the STATCOM as illustrated in the following Fig.20 beyond the digital PI controller, the direct axis, quadrature axis voltages again transformed into three phase voltages and used to generate the PWM pulses to the STATCOM in order to control its reactive power needed to control the terminal voltage. Fig.20 depicts the PV curves pf the system without and with open loop control of STATCOM, in which it is evident that the open loop control strategy of the STATCOM is well suitable to maintain almost constant voltages against inductive load variations. Hence, the open loop control strategy is more significant in controlling the terminal voltage with a constant value over a wide range of inductive or RL loads.

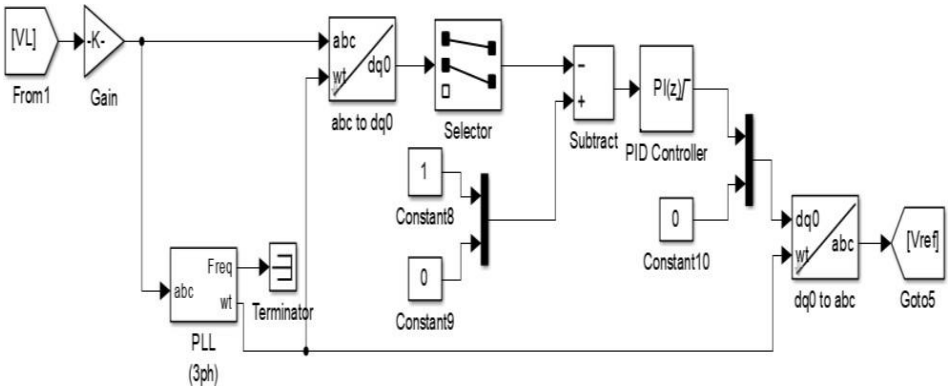

Figure.20. STATCOM Closed loop control circuit

The following part of this article presenting the result analysis of the closed loop control of the STATCOM for different inductive loads with a constant power factor of 0.89 lagging. Fig.21 depicts the voltage waveforms for RL Load 1, Fig.22 shows the voltage waveforms for RL Load 2, Fig.23 illustrates the voltage waveforms for RL Load 3 and Fig.24 represents the voltage waveforms for RL Load 4 with closed loop control of STATCOM. Table 3 encapsulates the terminal voltages of system with closed loop control of STATCOM. Fig.24 illustrates the PV curves of the system with closed loop control of STATCOM and Fig.25 shows the voltage bar chart of the corresponding system. This part of the result analysis proven the fact that even the closed loop control of the STATCOM is quite effective in improving the system voltage stability with voltage regulation with a specified band is quite suitable for SMLB systems with renewable sources.

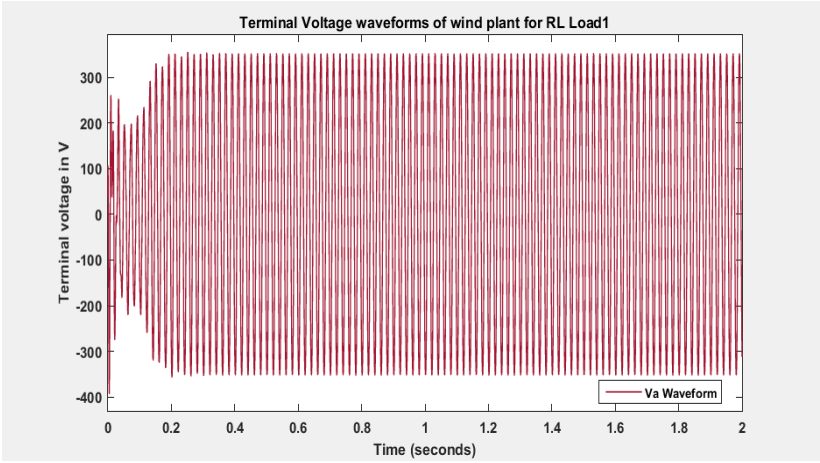

Figure.21. Voltage waveforms for RL Load 1 in closed loop control

References

1. P. Nakorn, P. Machot, V. Kinnares and C. Manop, "Study of Three-phase Self-excited Induction Generator Operating as Single-phase Induction Generator Supplying Non-linear Load," 2021 18th International Conference on Electrical Engineering/Electronics, Computer, Telecommunications and Information Technology (ECTI-CON), 2021, pp. 806-809, doi: 10.1109/ECTI-CON51831.2021.9454845.
2. M. G. B. Borja, S. Lescano, J. E. Luyo and U. Y. Tito, "MPPT of Three-Phase Self-Excited Induction Generator During Electric Power Generation from Variable Power Sources," 2021 1st International Conference on Power Electronics and Energy (ICPEE), 2021, pp. 1-6, doi: 10.1109/ICPEE50452.2021.9358538.
3. M. G. B. Borja, S. Lescano and J. E. Luyo, "Dynamic behavior of the wind turbine - self-exciting induction generator system, using a reference voltage of variable frequency as excitation," 2021 IEEE CHILEAN Conference on Electrical, Electronics Engineering, Information and Communication Technologies (CHILECON), 2021, pp. 1-6, doi: 10.1109/CHILECON54041.2021.9703069.
4. S. Chakraborty and R. Pudur, "Supply of Single-Phase Power for Rural Area using Three-Phase Self-Excited Induction Generator," 2021 Asian Conference on Innovation in Technology (ASIANCON), 2021, pp. 1-6, doi: 10.1109/ASIANCON51346.2021.9545057.
5. V. Yarlagadda, N. Alekhya, A. K. Garikapati, M. Gowrabathuni, K. Haritha and T. H. Rao, "Mitigation of Harmonics in WES Using Hybrid FACTS Controller," 2022 IEEE 2nd International Conference on Sustainable Energy and Future Electric Transportation (SeFeT), 2022, pp. 1-7, doi: 10.1109/SeFeT55524.2022.9908899.
6. C. Wu, X. -P. Zhang and M. Sterling, "Wind power generation variations and aggregations," in CSEE Journal of Power and Energy Systems, vol. 8, no. 1, pp. 17-38, Jan. 2022, doi: 10.17775/CSEEJPES.2021.03070.
7. V. Yarlagadda, A. K. Garikapati, N. Alekhya, M. Gowrabathuni, K. Haritha and T. H. Rao, "FFT Analysis and Harmonics Mitigation in WES using Multi-Level DSTATCOM," 2022 2nd Asian Conference on Innovation in Technology (ASIANCON), 2022, pp. 1-7, doi: 10.1109/ASIANCON55314.2022.9908927.
8. V. Yarlagadda, G. A. Karthika, M. Nagajyothi and J. Bhavani, "DSTATCOM based Closed Loop Controlled Wind Power Plant with Self Excited Induction Generator for Controlling

Terminal Voltage against Load Disturbances," 2022 IEEE Fourth International Conference on Advances in Electronics, Computers and Communications (ICAECC), 2022, pp. 1-6, doi: 10.1109/ICAECC54045.2022.9716651.

9. A. A. Ameri, M. B. Camara and B. Dakyo, "Efficient Energy Management for Wind-Battery Hybrid System Based Variable Frequency Approach," 2021 10th International Conference on Renewable Energy Research and Application (ICRERA), 2021, pp. 125-130, doi: 10.1109/ICRERA52334.2021.9598696.
10. O. Marchenko and S. Solomin, "Economic Efficiency of Solar and Wind Energy Joint Use in Autonomous Power Supply Systems on Lake Baikal Coast," 2021 International Ural Conference on Electrical Power Engineering (UralCon), 2021, pp. 101-105, doi: 10.1109/UralCon52005.2021.9559577.
11. M. W. Rahman, K. Velmurugan, M. S. Mahmud, A. Al Mamun and P. Ravindran, "Modelling of a stand- alone Wind-PV Hybrid Generation System Using (MATLAB/SIMULINK)," 2021 International Conference on Computing, Communication, and Intelligent Systems (ICCCIS), 2021, pp. 1000-1006, doi: 10.1109/ICCCIS51004.2021.9397194.
12. I. S. Rafiqi and A. H. Bhat, "Role of STATCOM in improving the power quality issues in hybrid power plant connected to a power grid," 2021 4th International Conference on Recent Developments in Control, Automation & Power Engineering (RDCAPE), 2021, pp. 384-387, doi: 10.1109/RDCAPE52977.2021.9633672.
13. Venu Yarlagadda, B. Devulal, Chava Sunil Kumar, Giriprasad Ambati, Srinivasa Rao Jalluri, Annapurna KarthikaGarikapati" Influence of Hybrid FACTS device and STATCOM on Power Quality Improvement of Wind Farm," Journal of Electrical Systems (JES) ISSN: 1112-5209, Vol. 20 No. 10s (2024): 104 - 115